# Rough volatility: An overview

Jim Gatheral

**Baruch**COLLEGE

WEISSMAN SCHOOL OF ARTS AND SCIENCES

**Master of Financial Engineering**

Financial Engineering Practitioners Seminar,
Columbia University,
Monday January 22, 2018

## Outline of this talk

- The term structure of the implied volatility skew
- A remarkable monofractal scaling property of historical volatility
- Fractional Brownian motion (fBm)
- The Rough Fractional Stochastic Volatility (RFSV) model
- Microstructural foundation
- The Rough Bergomi (rBergomi) model
- Fits to SPX
- Forecasting realized variance
- The Exponentiation Theorem and calibration

# The SPX volatility surface as of 15-Sep-2005



Figure 1: The SPX volatility surface as of 15-Sep-2005 (Figure 3.2 of The Volatility Surface).

## Term structure of at-the-money skew

- Given one smile for a fixed expiration, little can be said about the process generating it.
- In contrast, the dependence of the smile on time to expiration is intimately related to the underlying dynamics.
  - In particular model estimates of the term structure of ATM volatility skew defined as

$$\psi(\tau) := \left| \frac{\partial}{\partial k} \sigma_{\mathsf{BS}}(k, \tau) \right|_{k=0}.$$

  are very sensitive to the choice of volatility dynamics in a stochastic volatility model.

# Term structure of SPX ATM skew as of 15-Sep-2005
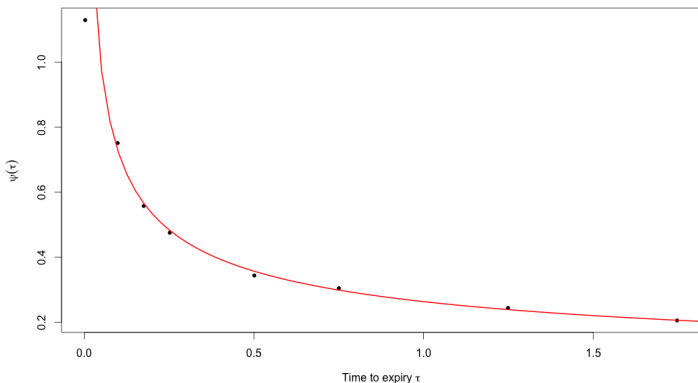


Figure 2: Term structure of ATM skew as of 15-Sep-2005, with power law fit $\tau^{-0.44}$ superimposed in red.

## Stylized facts

- Although the levels and orientations of the volatility surfaces change over time, their rough shape stays very much the same.
  - It's then natural to look for a time-homogeneous model.
- The term structure of ATM volatility skew

$$\psi(\tau) \sim \frac{1}{\tau^\alpha}$$

with $\alpha \in (0.3, 0.5)$.

## Motivation for Rough Volatility I: Better fitting stochastic volatility models

- Conventional stochastic volatility models generate volatility surfaces that are inconsistent with the observed volatility surface.
  - In stochastic volatility models, the ATM volatility skew is constant for short dates and inversely proportional to $T$ for long dates.
  - Empirically, we find that the term structure of ATM skew is proportional to $1/T^{\alpha}$ for some $0 < \alpha < 1/2$ over a very wide range of expirations.
- The conventional solution is to introduce more volatility factors, as for example in the DMR and Bergomi models.
  - One could imagine the power-law decay of ATM skew to be the result of adding (or averaging) many sub-processes, each of which is characteristic of a trading style with a particular time horizon.

## Bergomi Guyon

- Define the forward variance curve $\xi_t(u) = \mathbb{E}\left[v_u | \mathcal{F}_t\right]$.
- According to [BG12], in the context of a variance curve model, implied volatility may be expanded as

$$\sigma_{\mathrm{BS}}(k, T) = \sigma_0(T) + \sqrt{\frac{w}{T}} \frac{1}{2\,w^2}\, C^{x\xi}\, k + O(\eta^2) \qquad (1)$$

where $\eta$ is volatility of volatility, $w = \int_0^T \xi_0(s)\,ds$ is total variance to expiration $T$, and

$$C^{x\xi} = \int_0^T dt \int_t^T du\, \frac{\mathbb{E}\left[dx_t\, d\xi_t(u)\right]}{dt}. \qquad (2)$$

- Thus, given a stochastic volatility model written in forward variance form, we can easily (at least in principle) compute this smile approximation.

## The Bergomi model

- The $n$-factor Bergomi variance curve model reads:

$$\xi_t(u) = \xi_0(u) \exp\left\{ \sum_{i=1}^{n} \eta_i \int_0^t e^{-\kappa_i \,(t-s)} \, dW_s^{(i)} + \text{ drift } \right\}.$$
(3)

- The Bergomi model generates a term structure of volatility skew $\psi(\tau)$ that is something like

$$\psi(\tau) = \sum_i \frac{1}{\kappa_i \, \tau} \left\{ 1 - \frac{1 - e^{-\kappa_i \, \tau}}{\kappa_i \, \tau} \right\}.$$

  - This functional form is related to the term structure of the autocorrelation function.
  - Which is in turn driven by the exponential kernel in the exponent in (3).

## Tinkering with the Bergomi model

- Empirically, $\psi(\tau) \sim \tau^{-\alpha}$ for some $\alpha$.
- It's tempting to replace the exponential kernels in (3) with a power-law kernel.
- This would give a model of the form

$$\xi_t(u) = \xi_0(u) \exp\left\{ \eta \int_0^t \frac{dW_s}{(t-s)^\gamma} + \text{ drift} \right\}$$

which looks similar to

$$\xi_t(u) = \xi_0(u) \exp\left\{ \eta\, W_t^H + \text{ drift} \right\}$$

where $W_t^H$ is fractional Brownian motion.

## History of fractional stochastic volatility models

More formally, the model

$$\xi_t(u) = \xi_0(u) \exp \left\{ \eta \int_0^t \frac{dW_s}{(t-s)^\gamma} + \text{ drift} \right\}$$

belongs to a larger class of fractional stochastic volatility models that was originally shown by Alòs et al. in [ALV07] and then by Fukasawa in [Fuk11] to generate a short-dated ATM skew of the form

$$\psi(\tau) \sim \frac{1}{\tau^\gamma}$$

with $\gamma = \frac{1}{2} - H$ and $0 < H < \frac{1}{2}$.

# Motivation for Rough Volatility II: Power-law scaling of the historical volatility process

- The Oxford-Man Institute of Quantitative Finance makes historical realized variance (RV) estimates freely available at http://realized.oxford-man.ox.ac.uk. These estimates are updated daily.

- Using daily RV estimates as proxies for instantaneous variance, we may investigate the time series properties of $v_t$ empirically.
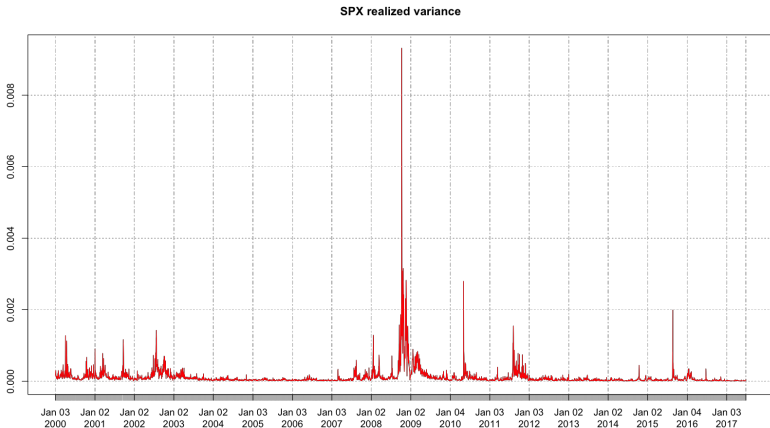
# SPX realized variance from 2000 to 2016



Figure 3:   KRV estimates of SPX realized variance from 2000 to 2017.

## The smoothness of the volatility process

- For $q \geq 0$, we define the $q$th sample moment of differences of log-volatility at a given lag $\Delta$[1]:

$$m(q, \Delta) = \langle |\log \sigma_{t+\Delta} - \log \sigma_t|^q \rangle$$

- For example

$$m(2, \Delta) = \langle (\log \sigma_{t+\Delta} - \log \sigma_t)^2 \rangle$$

  is just the sample variance of differences in log-volatility at the lag $\Delta$.

---

[1] $\langle \cdot \rangle$ denotes the sample average.
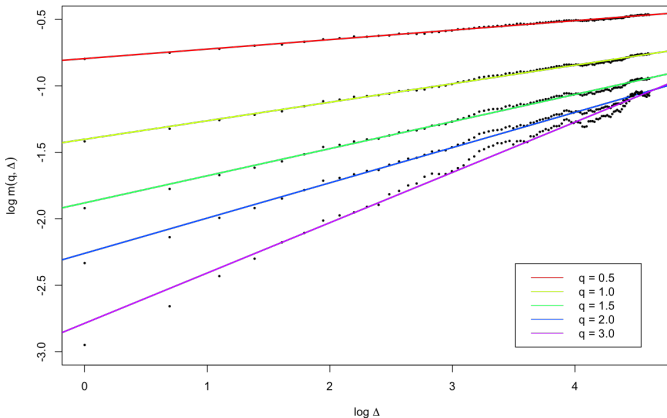
## Scaling of $m(q, \Delta)$ with lag $\Delta$



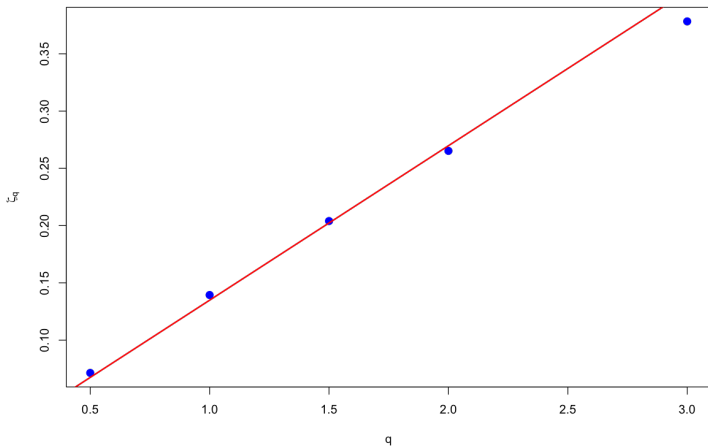Figure 4:  $\log m(q, \Delta)$ as a function of $\log \Delta$, SPX.

# Scaling of $\zeta_q$ with $q$



Figure 5: Scaling of $\zeta_q$ with $q$.

## Monofractal scaling result

- From the log-log plot Figure 4, we see that for each $q$, $m(q, \Delta) \propto \Delta^{\zeta_q}$.
- And from Figure 5 the monofractal scaling relationship

$$\zeta_q = q\,H$$

with $H \approx 0.13$.

  - Note also that our estimate of $H$ is biased high because we proxied instantaneous variance $v_t$ with its average over each day $\frac{1}{T} \int_0^T v_t\, dt$, where $T$ is one day.
  - On the other hand, the time series of realized variance is noisy and this causes our estimate of $H$ to be biased low.

- A time series of $H$ for SPX following the methodology of [BLP16] is shown in the next figure.

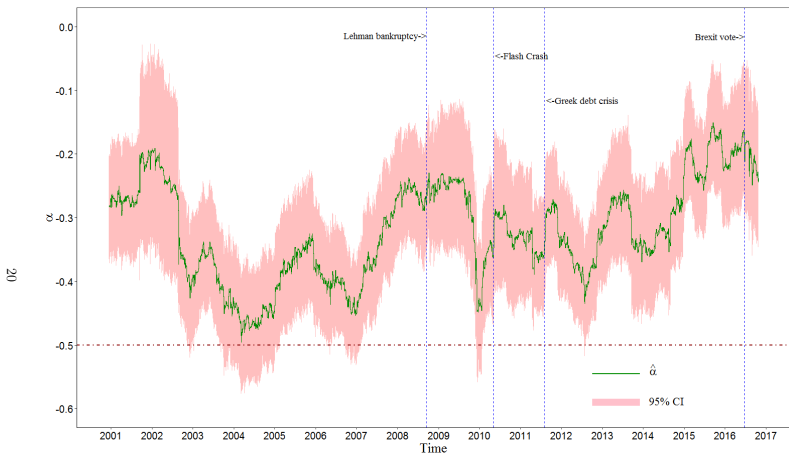# The time series of $\hat{\alpha} = H - \frac{1}{2}$ for SPX



Figure 10: Half year rolling-window estimates of $\alpha$ on the realized variance measures of the daily volatility by variogram OLS regression (3.10) with $m = 3$. The pink area is the 95% confidence interval by bootstrap method with $B = 999$. The four vertical dashed blue lines indicate four periods of market turmoil: Lehman Brothers filing for bankruptcy, the Flash Crash, the first bailout during Greek debt crisis and the Brexit referendum.

# Distributions of $(\log \sigma_{t+\Delta} - \log \sigma_t)$ for various lags $\Delta$
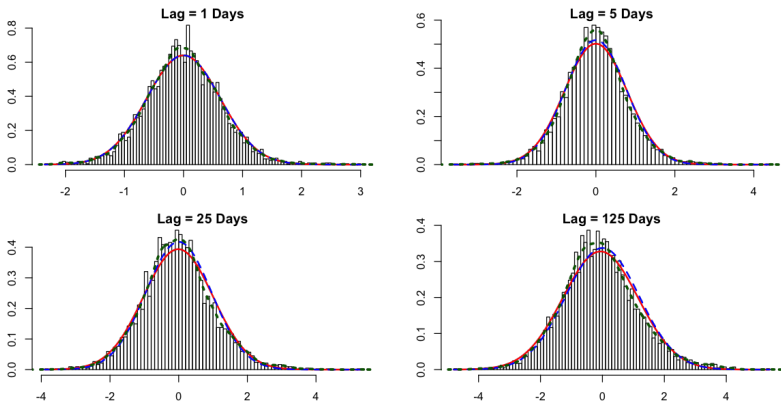


Figure 6: Histograms of $(\log \sigma_{t+\Delta} - \log \sigma_t)$ for various lags $\Delta$; normal fit in red; $\Delta = 1$ normal fit scaled by $\Delta^{0.14}$ in blue.

## Estimated $H$ for all indices

Estimating the relationship

$$\langle (\log \sigma_{t+\Delta} - \log \sigma_t)^2 \rangle = \nu^2 \, \Delta^{2\,H}$$

for all 21 indices in the Oxford-Man dataset yields:

| Index | $H$ | $\nu$ |
|---|---|---|
| SPX2.rk | 0.13 | 0.32 |
| FTSE2.rk | 0.14 | 0.27 |
| N2252.rk | 0.11 | 0.33 |
| GDAXI2.rk | 0.15 | 0.28 |
| RUT2.rk | 0.12 | 0.33 |
| AORD2.rk | 0.08 | 0.36 |
| DJI2.rk | 0.13 | 0.32 |
| IXIC2.rk | 0.13 | 0.30 |
| FCHI2.rk | 0.13 | 0.29 |
| HSI2.rk | 0.10 | 0.28 |
| KS11.rk | 0.12 | 0.28 |
| AEX.rk | 0.14 | 0.29 |
| SSMI.rk | 0.18 | 0.22 |
| IBEX2.rk | 0.13 | 0.28 |
| NSEI.rk | 0.11 | 0.32 |
| MXX.rk | 0.09 | 0.33 |
| BVSP.rk | 0.11 | 0.31 |
| GSPTSE.rk | 0.12 | 0.31 |
| STOXX50E.rk | 0.12 | 0.34 |
| FTSTI.rk | 0.13 | 0.23 |
| FTSEMIB.rk | 0.13 | 0.30 |

## Universality?

- In [GJR18], we compute daily realized variance estimates over one hour windows for DAX and Bund futures contracts, finding similar scaling relationships.
- We have also checked that Gold and Crude Oil futures scale similarly.
  - Although the increments ($\log \sigma_{t+\Delta} - \log \sigma_t$) seem to be fatter tailed than Gaussian.
- In [BLP16] Bennedsen et al., estimate volatility time series for more than five thousand individual US equities, finding rough volatility in every case.

## A natural model of realized volatility

- Distributions of differences in the log of realized volatility are close to Gaussian.
    - This motivates us to model $\sigma_t$ as a lognormal random variable.
- Moreover, the scaling property of variance of RV differences suggests the model:

$$\log \sigma_{t+\Delta} - \log \sigma_t = \nu \left( W_{t+\Delta}^H - W_t^H \right) \qquad (4)$$

    where $W^H$ is fractional Brownian motion.

- In [GJR18], we refer to a stationary version of (4) as the RFSV (for Rough Fractional Stochastic Volatility) model.

## Fractional Brownian motion (fBm)

- *Fractional Brownian motion* (fBm) $\{W_t^H; t \in \mathbb{R}\}$ is the unique Gaussian process with mean zero and autocovariance function

$$\mathbb{E}\left[W_t^H W_s^H\right] = \frac{1}{2}\left\{|t|^{2H} + |s|^{2H} - |t-s|^{2H}\right\}$$

  where $H \in (0,1)$ is called the *Hurst index* or parameter.
- In particular, when $H = 1/2$, fBm is just Brownian motion.
  - If $H > 1/2$, increments are positively correlated.
  - If $H < 1/2$, increments are negatively correlated.

## Apparent fractality of the volatility time series
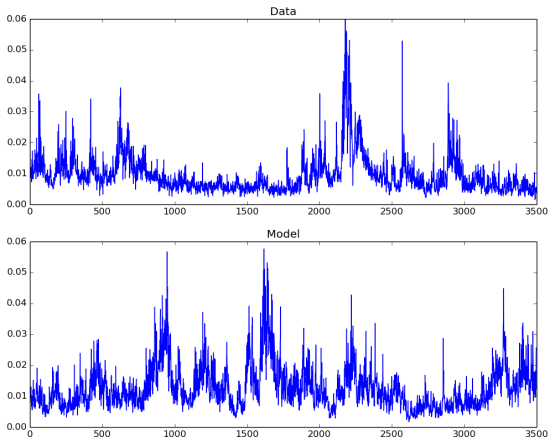


Figure 7:   Volatility of SPX (above) and in the RFSV model (below).

## Remarks on the comparison

- The qualitative features of simulated and actual graphs look very similar.
  - Persistent periods of high volatility alternate with low volatility periods.
- $H \sim 0.1$ generates very rough looking sample paths (compared with $H = 1/2$ for Brownian motion).
  - Hence *rough volatility*.
- On closer inspection, we observe fractal-type behavior.
  - The graph of volatility over a small time period looks like the same graph over a much longer time period.
- This feature of volatility has been investigated both empirically and theoretically in, for example, [BM03].
  - In particular, their Multifractal Random Walk (MRW) is related to a limiting case of the RSFV model as $H \to 0$.

# Microstructural foundation for rough volatility

In [JR16], El Euch, Fukasawa and Rosenbaum consider a
generalization of a simple model of price dynamics in terms of
Hawkes processes due to Bacry et al. ([BM14]) with the following
properties:

- Reflecting the high degree of endogeneity of the market, the
  $L^1$ norm of the kernel matrix is close to one (nearly unstable).
- No drift in the price process imposes a relationship between
  buy and sell kernels.
- Liquidity asymmetry: The average impact of a sell order is
  greater than the impact of a buy order.
- Splitting of metaorders motivates power-law decay of the
  Hawkes kernels $\varphi(\tau) \sim \tau^{-(1+\alpha)}$ (empirically $\alpha \approx 0.6$).

## The scaling limit of the price model

They construct a sequence of such Hawkes processes suitably rescaled in time and space that converges in law to a Rough Heston process of the form

$$
\begin{aligned}
\frac{dS_t}{S_t} &= \sqrt{v_t}\, dZ_t \\
v_t &= v_0 + \frac{\lambda}{\Gamma(\alpha)} \int_0^t \frac{\theta - v_s}{(t-s)^{1-\alpha}}\, ds + \frac{\lambda\nu}{\Gamma(\alpha)} \int_0^t \frac{\sqrt{v_s}\, dW_s}{(t-s)^{1-\alpha}}
\end{aligned}
$$

with

$$
d\langle Z, W \rangle_t = \rho\, dt.
$$

- The correlation $\rho$ is related to a liquidity asymmetry parameter.
- Rough volatility can thus be understood as relating to the persistence of order flow and the high degree of endogeneity of liquid markets.

## The Rough Heston characteristic function

Define the fractional integral and differential operators:

$$I^{1-\alpha}f(t) = \frac{1}{\Gamma(1-\alpha)} \int_0^t \frac{f(s)}{(t-s)^\alpha}\, ds; \quad D^\alpha f(t) = \frac{d}{dt}\, I^{1-\alpha}f(t).$$

Remarkably, in [ER16], El Euch and Rosenbaum compute the following expression for the characteristic function of the Rough Heston model:

$$\phi_t(u) = \exp\left\{\theta\,\lambda \int_0^t h(u,s)\, ds + v_0\, I^{1-\alpha}h(u,t)\right\}$$

where $h(u,)$ solves the fractional Riccati equation

$$D^\alpha h(u,s) = -\frac{1}{2}\, u\,(u+i) + \lambda\,(i\,\rho\,\nu\,u - 1)\, h(u,s) + \frac{(\lambda\,\nu)^2}{2}\, h^2(u,s).$$

## The forecast formula

- In the RFSV model (4), $\log v_t \approx 2\,\nu\,W_t^H + C$ for some constant $C$.
- [NP00] show that $W_{t+\Delta}^H$ is conditionally Gaussian with conditional expectation

$$\mathbb{E}[W_{t+\Delta}^H|\mathcal{F}_t] = \frac{\cos(H\pi)}{\pi}\Delta^{H+1/2}\int_{-\infty}^t \frac{W_s^H}{(t-s+\Delta)(t-s)^{H+1/2}}\,ds$$

and conditional variance

$$\text{Var}[W_{t+\Delta}^H|\mathcal{F}_t] = c\,\Delta^{2H}.$$

where

$$c = \frac{\Gamma(3/2-H)}{\Gamma(H+1/2)\,\Gamma(2-2H)}.$$

## The forecast formula

- Thus, we obtain

---

### Variance forecast formula

$$\mathbb{E}^{\mathbb{P}}\left[v_{t+\Delta}|\,\mathcal{F}_t\right] = \exp\left\{\mathbb{E}^{\mathbb{P}}\left[\log(v_{t+\Delta})|\,\mathcal{F}_t\right] + 2\,c\,\nu^2\Delta^{2H}\right\} \quad (5)$$

---

where

$$\mathbb{E}^{\mathbb{P}}\left[\log v_{t+\Delta}|\,\mathcal{F}_t\right]$$
$$= \frac{\cos(H\pi)}{\pi}\Delta^{H+1/2}\int_{-\infty}^{t}\frac{\log v_s}{(t-s+\Delta)(t-s)^{H+1/2}}ds.$$

- [BLP16] confirm that this forecast outperforms the best performing existing alternatives such as HAR, at least at daily or higher timescales.

## Pricing under rough volatility

Once again, the data suggests the following model for volatility under the real (or historical or physical) measure $\mathbb{P}$:

$$\log \sigma_t = \nu \, W_t^H.$$

Let $\gamma = \frac{1}{2} - H$. We choose the Mandelbrot-Van Ness representation of fractional Brownian motion $W^H$ as follows:

$$W_t^H = C_H \left\{ \int_{-\infty}^t \frac{dW_s^{\mathbb{P}}}{(t-s)^\gamma} - \int_{-\infty}^0 \frac{dW_s^{\mathbb{P}}}{(-s)^\gamma} \right\}$$

where the choice

$$C_H = \sqrt{\frac{2 H \, \Gamma(3/2 - H)}{\Gamma(H + 1/2) \, \Gamma(2 - 2 H)}}$$

ensures that

$$\mathbb{E}\left[ W_t^H \, W_s^H \right] = \frac{1}{2} \left\{ t^{2H} + s^{2H} - |t - s|^{2H} \right\}.$$

## Pricing under rough volatility

Then

$$\log v_u - \log v_t$$
$$= \nu\, C_H \left\{ \int_t^u \frac{1}{(u-s)^\gamma}\, dW_s^{\mathbb{P}} + \int_{-\infty}^t \left[ \frac{1}{(u-s)^\gamma} - \frac{1}{(t-s)^\gamma} \right] dW_s^{\mathbb{P}} \right\}$$
$$=: 2\,\nu\, C_H \left[ M_t(u) + Z_t(u) \right]. \tag{6}$$

- Note that $\mathbb{E}^{\mathbb{P}}\left[ M_t(u) \middle| \mathcal{F}_t \right] = 0$ and $Z_t(u)$ is $\mathcal{F}_t$-measurable.
- To price options, it would seem that we would need to know $\mathcal{F}_t$, the entire history of the Brownian motion $W_s$ for $s < t$!

## Pricing under $\mathbb{P}$

Let

$$\tilde{W}_t^{\mathbb{P}}(u) := \sqrt{2\,H} \int_t^u \frac{dW_s^{\mathbb{P}}}{(u-s)^\gamma}$$

With $\eta := 2\,\nu\,C_H/\sqrt{2\,H}$ we have $2\,\nu\,C_H\,M_t(u) = \eta\,\tilde{W}_t^{\mathbb{P}}(u)$ so denoting the stochastic exponential by $\mathcal{E}(\cdot)$, we may write

$$
\begin{aligned}
v_u &= v_t \exp\left\{\eta\tilde{W}_t^{\mathbb{P}}(u) + 2\,\nu\,C_H\,Z_t(u)\right\} \\
&= \mathbb{E}^{\mathbb{P}}\left[v_u|\,\mathcal{F}_t\right]\,\mathcal{E}\left(\eta\,\tilde{W}_t^{\mathbb{P}}(u)\right).
\end{aligned}
\tag{7}
$$

- The conditional distribution of $v_u$ depends on $\mathcal{F}_t$ only through the variance forecasts $\mathbb{E}^{\mathbb{P}}\left[v_u|\,\mathcal{F}_t\right]$,
- To price options, one does not need to know $\mathcal{F}_t$, the entire history of the Brownian motion $W_s^{\mathbb{P}}$ for $s < t$.

## Pricing under $\mathbb{Q}$

Our model under $\mathbb{P}$ reads:

$$v_u = \mathbb{E}^{\mathbb{P}}\left[v_u | \mathcal{F}_t\right] \mathcal{E}\left(\eta\, \tilde{W}_t^{\mathbb{P}}(u)\right). \tag{8}$$

Consider some general change of measure

$$dW_s^{\mathbb{P}} = dW_s^{\mathbb{Q}} + \lambda_s\, ds,$$

where $\{\lambda_s : s > t\}$ has a natural interpretation as the price of volatility risk. We may then rewrite $(8)$ as

$$v_u = \mathbb{E}^{\mathbb{P}}\left[v_u | \mathcal{F}_t\right] \mathcal{E}\left(\eta\, \tilde{W}_t^{\mathbb{Q}}(u)\right) \exp\left\{\eta\sqrt{2\,H} \int_t^u \frac{\lambda_s}{(u-s)^\gamma}\, ds\right\}.$$

- Although the conditional distribution of $v_u$ under $\mathbb{P}$ is lognormal, it will not be lognormal in general under $\mathbb{Q}$.
  - The upward sloping smile in VIX options means $\lambda_s$ cannot be deterministic in this picture.

## The rough Bergomi (rBergomi) model

Let's nevertheless consider the simplest change of measure

$$dW_s^{\mathbb{P}} = dW_s^{\mathbb{Q}} + \lambda(s)\,ds,$$

where $\lambda(s)$ is a deterministic function of $s$. Then from (34), we would have

$$
\begin{aligned}
v_u &= \mathbb{E}^{\mathbb{P}}\left[v_u|\,\mathcal{F}_t\right]\mathcal{E}\left(\eta\,\tilde{W}_t^{\mathbb{Q}}(u)\right)\exp\left\{\eta\,\sqrt{2H}\int_t^u\frac{1}{(u-s)^{\gamma}}\,\lambda(s)\,ds\right\} \\
&= \xi_t(u)\,\mathcal{E}\left(\eta\,\tilde{W}_t^{\mathbb{Q}}(u)\right)
\end{aligned}
\tag{9}
$$

where the forward variances $\xi_t(u) = \mathbb{E}^{\mathbb{Q}}\left[v_u|\,\mathcal{F}_t\right]$ are (at least in principle) tradable and observed in the market.

- $\xi_t(u)$ is the product of two terms:
  - $\mathbb{E}^{\mathbb{P}}\left[v_u|\,\mathcal{F}_t\right]$ which depends on the historical path $\{W_s, s < t\}$ of the Brownian motion
  - a term which depends on the price of risk $\lambda(s)$.

## Features of the rough Bergomi model

- The rBergomi model is a non-Markovian generalization of the Bergomi model:

$$\mathbb{E}\left[v_u|\,\mathcal{F}_t\right] \neq \mathbb{E}[v_u|v_t].$$

- The rBergomi model is Markovian in the (infinite-dimensional) state vector $\mathbb{E}^{\mathbb{Q}}\left[v_u|\,\mathcal{F}_t\right] = \xi_t(u)$.

- We have achieved our aim of replacing the exponential kernels in the Bergomi model (3) with a power-law kernel.
  - We may therefore expect that the rBergomi model will generate a realistic term structure of ATM volatility skew.

## The stock price process

- The observed anticorrelation between price moves and volatility moves may be modeled naturally by anticorrelating the Brownian motion $W$ that drives the volatility process with the Brownian motion driving the price process.

- Thus

$$\frac{dS_t}{S_t} = \sqrt{v_t}\, dZ_t$$

with

$$dZ_t = \rho\, dW_t + \sqrt{1 - \rho^2}\, dW_t^{\perp}$$

where $\rho$ is the correlation between volatility moves and price moves.

## Hybrid simulation of BSS processes

- In [BFG16], we simulate the rBergomi model by generating paths of $\tilde{W}$ and $Z$ with the correct joint marginals using Cholesky decomposition.

  - This is very slow!

- The rBergomi variance process is a special case of a Brownian Semistationary (BSS) process.

- In [BLP17], Bennedsen et al. show how to simulate such processes more efficiently.

  - Their hybrid BSS scheme is much more efficient than the exact simulation described above.
  - An even more efficient scheme is presented in [MP17].
  - However, it is still not fast enough to enable efficient calibration of the Rough Bergomi model to the volatility surface.

## Guessing rBergomi model parameters

- The rBergomi model has only three parameters: $H$, $\eta$ and $\rho$.
- These parameters have very direct interpretations:
    - $H$ controls the decay of ATM skew $\psi(\tau)$ for very short expirations
    - The product $\rho\,\eta$ sets the level of the ATM skew for longer expirations.
    - Keeping $\rho\,\eta$ constant but decreasing $\rho$ (so as to make it more negative) pushes the minimum of each smile towards higher strikes.
- So we can guess parameters in practice.

## SPX smiles in the rBergomi model

- In Figure 9, we show how well a rBergomi model simulation
  with guessed parameters fits the SPX option market as of
  August 14, 2013, one trading day before the third Friday
  expiration.
  - Options set at the open of August 16, 2013 so only one
    trading day left.
- rBergomi parameters were: $H = 0.05$, $\eta = 2.3$, $\rho = -0.9$.
  - Only three parameters to get a very good fit to the whole SPX
    volatility surface!
- Note in particular that the extreme short-dated smile is well
  reproduced by the rBergomi model.
  - There is no need to add jumps!

# SPX smiles as of August 14, 2013
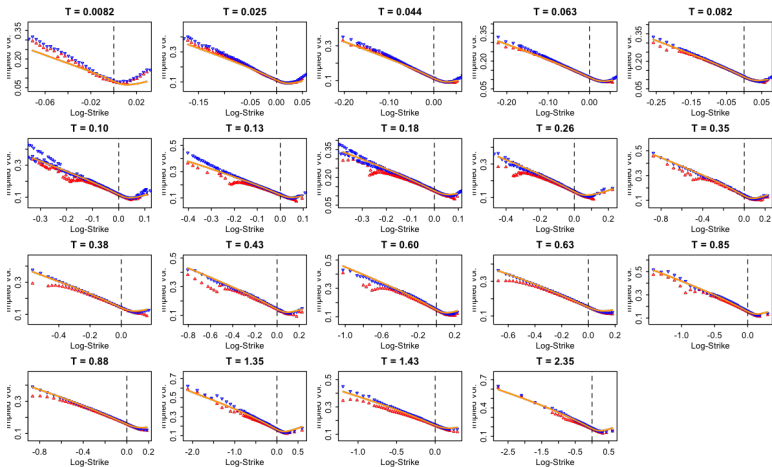


Figure 8: Red and blue points represent bid and offer SPX implied volatilities; orange smiles are from the rBergomi simulation.

# The one-month SPX smile as of August 14, 2013
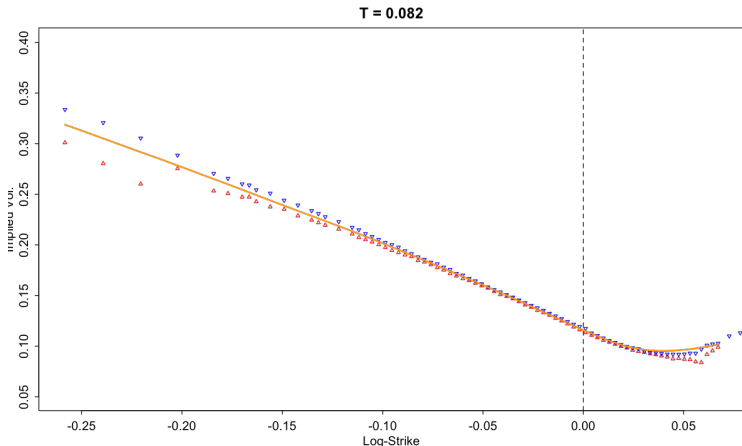


Figure 9: Red and blue points represent bid and offer SPX implied volatilities; the orange smiles is from the rBergomi simulation.

## ATM volatilities and skews

In Figures 10 and 11, we see just how well the rBergomi model can match empirical ATM vols and skews. Recall also that the parameters we used are just guesses!

## Term structure of ATM vol as of August 14, 2013
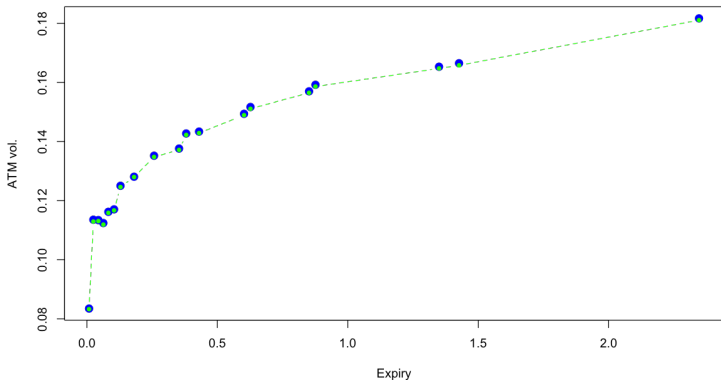


Figure 10: Blue points are empirical ATM volatilities; green points are from the rBergomi simulation. The two match very closely, as they should.

# Term structure of ATM skew as of August 14, 2013
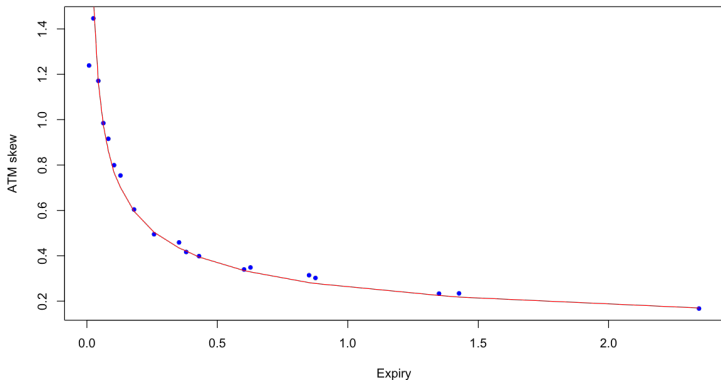


Figure 11: Blue points are empirical skews; the red line is from the rBergomi simulation.

## Calibration

- As mentioned earlier, computation in the rBergomi model is challenging so calibration is not easy.
    - Though as noted earlier, we can easily guess parameters.
- We have investigated a number of approaches to calibration
    - Asymptotic expansions
    - Chebyshev interpolation
    - Moment matching
- So far, we cannot claim to have had real success with any of these approaches.
- A recent development shows some promise however...

## The Alòs Itô decomposition formula

Following Elisa Alòs in [Alò12], let $X_t = \log S_t / K$ and consider the price process

$$dX_t = \sigma_t \, dZ_t - \frac{1}{2} \, \sigma_t^2 \, dt.$$

Now let $H(x, w)$ be some function that solves the Black-Scholes equation.

- Specifically,

$$-\partial_w H(x, w) + \frac{1}{2} \, (\partial_{xx} - \partial_x) \, H(x, w) = 0$$

which is of course the gamma-vega relationship.

- Note in particular that $\partial_x$ and $\partial_w$ commute when applied to a solution of the Black-Scholes equation.

Now, define $w_t(T)$ as the integral of the expected future variance:

$$w_t(T) := \mathbb{E}\left[\left. \int_t^T \sigma_s^2 ds \right| \mathcal{F}_t \right].$$

Notice that

$$w_t(T) = M_t - \int_0^t \sigma_s^2 ds,$$

where the martingale $M_t := \mathbb{E}\left[\left. \int_0^T \sigma_s^2 ds \right| \mathcal{F}_t \right]$. Then it follows that

$$dw_t(T) = -\sigma_t^2 \, dt + dM_t.$$

Applying Itô's Lemma to $H_t := H(X_t, w_t(T))$, taking conditional expectations, simplifying using the Black-Scholes equation and integrating, we obtain

---

**Theorem (The Itô Decomposition Formula of Alòs)**

$$
\begin{aligned}
\mathbb{E}\left[H_T \mid \mathcal{F}_t\right] = {} & H_t + \mathbb{E}\left[\left. \int_t^T \partial_{xw} H_s \, d\langle X, M \rangle_s \right| \mathcal{F}_t\right] \\
& + \frac{1}{2} \mathbb{E}\left[\left. \int_t^T \partial_{ww} H_s \, d\langle M, M \rangle_s \right| \mathcal{F}_t\right]. \tag{10}
\end{aligned}
$$

---

- Note in particular that (10) is an *exact* decomposition.

## Freezing derivatives

Freezing the derivatives in the Alòs Itô decomposition formula (10) gives us the approximation

$$
\begin{aligned}
\mathbb{E}\left[H_T \middle| \mathcal{F}_t\right] &\approx H_t + \mathbb{E}\left[\int_t^T d\langle X, M\rangle_s \middle| \mathcal{F}_t\right] \partial_{xw} H_t \\
&\quad + \frac{1}{2}\mathbb{E}\left[\int_t^T d\langle M, M\rangle_s \middle| \mathcal{F}_t\right] \partial_{ww} H_t \\
&= H_t + (X \diamond M)_t(T) \cdot H_t + \frac{1}{2}(M \diamond M)_t(T) \cdot H_t.
\end{aligned}
$$

### Remark

The essence of the Exponentiation Theorem is that we may express $\mathbb{E}\left[H_T \middle| \mathcal{F}_t\right]$ as an exact expansion consisting of infinitely many terms, with derivatives in each such term frozen.

## Diamond and dot notation

Let $A_t$ and $B_t$ be stochastic processes (some combinations of $X_t$ and $M_t$). Then

$$(A \diamond B)_t(T) = \mathbb{E}\left[\int_t^T d\langle A, B\rangle_s \,\bigg|\, \mathcal{F}_t\right].$$

When $(A \diamond B)_t(T)$ appears before some solution $H_t$ of the Black-Scholes equation, the dot $\cdot$ is to be understood as representing the action of $\partial_x$ and $\partial_w$ applied to $H_t$.

So for example

$$(X \diamond M)_t(T) \cdot H_t \;=\; \mathbb{E}\left[\int_t^T d\langle X, M\rangle_s \,\bigg|\, \mathcal{F}_t\right] \partial_{xw} H_t$$

and so on.

## Trees

- Terms such as $(X \diamond M)$, $(M \diamond M)$ and $X \diamond (X \diamond M)$ are naturally indexed by trees, each of whose leaves corresponds to either $X$ or $M$.

- We end up with diamond trees reminiscent of Feynman diagrams, with analogous rules.

## Forests

### Definition

Let $\mathbb{F}_0 = M$. Then the higher order forests $\mathbb{F}_k$ are defined recursively as follows:

$$\mathbb{F}_k = \frac{1}{2} \sum_{i,j=0}^{k-2} \mathbb{1}_{i+j=k-2}\, \mathbb{F}_i \diamond \mathbb{F}_j + X \diamond \mathbb{F}_{k-1}.$$

## The first few forests

Applying this definition to compute the first few terms, we obtain

$$
\begin{aligned}
\mathbb{F}_0 &= M \\
\mathbb{F}_1 &= X \diamond \mathbb{F}_0 = (X \diamond M) \\
\mathbb{F}_2 &= \frac{1}{2}(\mathbb{F}_0 \diamond \mathbb{F}_0) + X \diamond \mathbb{F}_1 = \frac{1}{2}(M \diamond M) + X \diamond (X \diamond M) \\
\mathbb{F}_3 &= (\mathbb{F}_0 \diamond \mathbb{F}_1) + X \diamond \mathbb{F}_2 \\
&= M \diamond (X \diamond M) + \frac{1}{2} X \diamond (M \diamond M) + X \diamond (X \diamond (X \diamond M))
\end{aligned}
$$

## The first forest $\mathbb{F}_1 = X \diamond M$
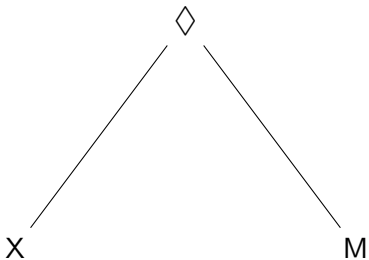
## The second forest $\mathbb{F}_2$

$$\mathbb{F}_2 = \frac{1}{2}(M \diamond M) + X \diamond (X \diamond M)$$

## The third forest $\mathbb{F}_3$

$$\mathbb{F}_3 = M \diamond (X \diamond M) + \frac{1}{2} X \diamond (M \diamond M) + X \diamond (X \diamond (X \diamond M))$$
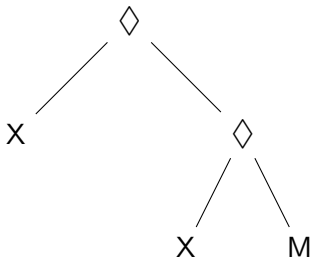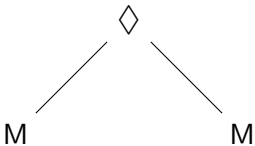
## Simple diamond rules

- For $k > 0$, the $k$th forest $\mathbb{F}_k$ contains all trees with $k + 2$ leaves where $X$ is counted as a single leaf, and $M$ as a double leaf.
- Prefactor computation:
  - Work from the bottom up.
  - If child subtrees immediately below a diamond node are identical, carry a multiplicative factor of $\frac{1}{2}$.

## The Exponentiation Theorem

The following theorem proved in [AGR17] follows from (more or less) a simple application of Itô's Lemma and the Alòs Itô decomposition formula.

### Theorem

*Let $H_t$ be any solution of the Black-Scholes equation such that $\mathbb{E}\left[H_T | \mathcal{F}_t\right]$ is finite and the integrals contributing to each forest $\mathbb{F}_k, k \geq 0$ exist. Then*

$$\mathbb{E}\left[H_T | \mathcal{F}_t\right] = e^{\sum_{k=1}^{\infty} \mathbb{F}_k} \cdot H_t.$$

## If $H_t$ is a characteristic function

Consider the Black-Scholes characteristic function

$$\Phi_t^T(a) = e^{i\, a\, X_t - \frac{1}{2} a\, (a+i)\, w_t(T)}$$

which satisfies the Black-Scholes equation.

- Applying $\mathbb{F}_k$ to $\Phi$ just multiplies $\Phi$ by some deterministic factor.
- Then
$$e^{\sum_{k=1}^{\infty} \mathbb{F}_k} \cdot \Phi_t^T(a) = e^{\sum_{k=1}^{\infty} \tilde{\mathbb{F}}_k(a)}\, \Phi_t^T(a)$$

  where $\tilde{\mathbb{F}}_k(a)$ is $\mathbb{F}_k$ with each occurrence of $\partial_x$ replaced with $i\, a$ and each occurrence of $\partial_w$ replaced with $-\frac{1}{2}\, a\, (a+i)$.

Then from the Exponentiation Theorem, we have the following lemma.

### Lemma

*Let*

$$\varphi_t^T(a) = \mathbb{E}\left[ e^{i\,a\,X_T} \,\middle|\, \mathcal{F}_t \right]$$

*be the characteristic function of the log stock price. Then*

$$\varphi_t^T(a) = e^{\sum_{k=1}^{\infty} \tilde{\mathbb{F}}_k(a)}\, \Phi_t^T(a).$$

### Corollary

The cumulant generating function (CGF) is given by

$$\psi_t^T(a) = \log \varphi_t^T(a) = i\,a\,X_t - \frac{1}{2}a\,(a+i)\,w_t(T) + \sum_{k=1}^{\infty} \tilde{\mathbb{F}}_k(a).$$

## Variance and gamma swaps

The variance swap is given by the fair value of the log-strip:

$$\mathbb{E}\left[X_T | \mathcal{F}_t\right] = (-\mathrm{i})\,\psi_t^{T'}(0) = X_t - \frac{1}{2}\,w_t(T)$$

and the gamma swap (wlog set $X_t = 0$) by

$$\mathbb{E}\left[X_T\,e^{X_T} \middle| \mathcal{F}_t\right] = -\mathrm{i}\,\psi_t^{T'}(-\mathrm{i}).$$

### Remark

The point is that we can in principle compute such moments for any stochastic volatility model written in forward variance form, whether or not there exists a closed-form expression for the characteristic function.

## The gamma swap

It is easy to see that only trees containing a single $M$ leaf will survive in the sum after differentiation when $a = -\mathrm{i}$ so that

$$\sum_{k=1}^{\infty} \tilde{\mathbb{F}}'_k(-\mathrm{i}) = \frac{\mathrm{i}}{2} \sum_{k=1}^{\infty} (X\diamond)^k M$$

where $(X\diamond)^k M$ is defined recursively for $k > 0$ as $(X\diamond)^k M = X \diamond (X\diamond)^{k-1} M$. Then the fair value of a gamma swap is given by

$$\mathcal{G}_t(T) = 2\,\mathbb{E}\left[ X_T\, e^{X_T} \,\middle|\, \mathcal{F}_t \right] = w_t(T) + \sum_{k=1}^{\infty} (X\diamond)^k M. \qquad (11)$$

### Remark

Equation (11) allows for explicit computation of the gamma swap for any model written in forward variance form.

## The leverage swap

We deduce that the fair value of a leverage swap is given by

$$\mathcal{L}_t(T) = \mathcal{G}_t(T) - w_t(T) = \sum_{k=1}^{\infty} (X\diamond)^k M. \tag{12}$$

- The leverage swap is expressed explicitly in terms of covariance functionals of the spot and vol. processes.
  - If spot and vol. processes are uncorrelated, the fair value of the leverage swap is zero.

An explicit expression for the leverage swap!

## Leverage swap from the smile

Let
$$d_\pm(k) = \frac{-k}{\sigma_{\mathrm{BS}}(k, T)\sqrt{T}} \pm \frac{\sigma_{\mathrm{BS}}(k, T)\sqrt{T}}{2}$$

and following Fukasawa in [Fuk12], denote the inverse functions by $g_\pm(z) = d_\pm^{-1}(z)$. Further define

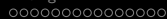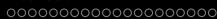$$\sigma_\pm(z) = \sigma_{\mathrm{BS}}(g_\pm(z), T)\sqrt{T}.$$

- Then the variance swap may be estimated from the smile using

$$w_t(T) = \int_{\mathbb{R}} dz \, N'(z) \, \sigma_-^2(z).$$

- And the gamma swap may be estimated using

$$\mathcal{G}_t(T) = \int_{\mathbb{R}} dz \, N'(z) \, \sigma_+^2(z).$$

- Recall that $\mathcal{L}_t(T) = \mathcal{G}_t(T) - w_t(T)$.

- We may thus compute leverage swaps in any stochastic volatility model (in principle) and also estimate leverage swaps from the implied volatility surface.
  - Model calibration is possible!
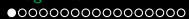
## The rough Heston model

In the zero mean reversion limit, the rough Heston model of [ER16] may be written as

$$\frac{dS_t}{S_t} = \sqrt{v_t} \left\{ \rho \, dW_t + \sqrt{1 - \rho^2} \, dW_t^\perp \right\} = \sqrt{v_t} \, dZ_t$$

with

$$v_u = \xi_t(u) + \frac{\nu}{\Gamma(\alpha)} \int_t^u \frac{\sqrt{v_s}}{(u-s)^\gamma} \, dW_s, \quad u \geq t$$

where $\xi_t(u) = \mathbb{E}\left[ v_u | \mathcal{F}_t \right]$ is the forward variance curve, $\gamma = \frac{1}{2} - H$ and $\alpha = 1 - \gamma = H + \frac{1}{2}$.

## The rough Heston model in forward variance form

In forward variance form,

$$d\xi_t(u) = \frac{\nu}{\Gamma(\alpha)} \frac{\sqrt{v_t}}{(u-t)^\gamma} \, dW_t. \tag{13}$$

### Remark

(13) is a natural fractional generalization of the classical Heston model which reads, in forward variance form [BG12],

$$d\xi_t(u) = \nu \sqrt{v_t} \, e^{-\kappa(u-t)} \, dW_t.$$

## Computation of autocovariance functionals

Apart from $\mathcal{F}_t$ measurable terms (abbreviated as 'drift'), we have

$$
\begin{aligned}
dX_t &= \sqrt{v_t}\, dZ_t + \text{drift} \\
dM_t &= \int_t^T d\xi_t(u)\, du \\
&= \frac{\nu}{\Gamma(\alpha)}\, \sqrt{v_t} \left( \int_t^T \frac{du}{(u-t)^\gamma} \right)\, dW_t \\
&= \frac{\nu\,(T-t)^\alpha}{\Gamma(1+\alpha)}\, \sqrt{v_t}\, dW_t.
\end{aligned}
$$

## The first order forest

There is only one tree in the forest $\mathbb{F}_1$.

$$
\begin{aligned}
\mathbb{F}_1 = (X \diamond M)_t(T) &= \mathbb{E}\left[\int_t^T d\langle X, M\rangle_s \,\middle|\, \mathcal{F}_t\right] \\
&= \frac{\rho\,\nu}{\Gamma(1+\alpha)} \,\mathbb{E}\left[\int_t^T v_s\,(T-s)^\alpha\,ds \,\middle|\, \mathcal{F}_t\right] \\
&= \frac{\rho\,\nu}{\Gamma(1+\alpha)} \int_t^T \xi_t(s)\,(T-s)^\alpha\,ds.
\end{aligned}
$$

## Higher order forests

Define for $j \geq 0$

$$I_t^{(j)}(T) := \int_t^T ds\, \xi_t(s)\, (T-s)^{j\alpha}.$$

Then

$$\begin{aligned}
dI_s^{(j)}(T) &= \int_s^T du\, d\xi_s(u)\, (T-u)^{j\alpha} + \text{ drift terms} \\
&= \frac{\nu\sqrt{v_s}}{\Gamma(\alpha)}\, dW_s \int_s^T \frac{(T-u)^{j\alpha}}{(u-s)^\gamma}\, du + \text{ drift terms} \\
&= \frac{\Gamma(1+j\alpha)}{\Gamma(1+(j+1)\alpha)}\, \nu\sqrt{v_s}\, (T-s)^{(j+1)\alpha}\, dW_s + \text{ drift terms}.
\end{aligned}$$

With this notation,

$$(X \diamond M)_t(T) = \frac{\rho\,\nu}{\Gamma(1+\alpha)}\, I_t^{(1)}(T).$$

## The second order forest

There are two trees in $\mathbb{F}_2$:

$$
\begin{aligned}
(M \diamond M)_t(T) &= \mathbb{E}\left[\int_t^T d\langle M, M\rangle_s \,\middle|\, \mathcal{F}_t\right] \\
&= \frac{\nu^2}{\Gamma(1+\alpha)^2} \int_t^T \xi_t(s)\,(T-s)^{2\alpha}\,ds \\
&= \frac{\nu^2}{\Gamma(1+\alpha)^2}\, I_t^{(2)}(T)
\end{aligned}
$$

and

$$
\begin{aligned}
(X \diamond (X \diamond M))_t(T) &= \frac{\rho\,\nu}{\Gamma(1+\alpha)} \mathbb{E}\left[\int_t^T d\langle X, I^{(1)}\rangle_s \,\middle|\, \mathcal{F}_t\right] \\
&= \frac{\rho^2\,\nu^2}{\Gamma(1+2\,\alpha)}\, I_t^{(2)}(T).
\end{aligned}
$$

## The third order forest

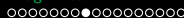Continuing to the forest $\mathbb{F}_3$, we have the following.

$$
\begin{aligned}
(M \diamond (X \diamond M))_t (T) &= \frac{\rho\,\nu^3}{\Gamma(1+\alpha)\,\Gamma(1+2\,\alpha)}\, I_t^{(3)}(T) \\
(X \diamond (X \diamond (X \diamond M)))_t (T) &= \frac{\rho^3\,\nu^3}{\Gamma(1+3\,\alpha)}\, I_t^{(3)}(T) \\
(X \diamond (M \diamond M))_t (T) &= \frac{\rho\,\nu^3\,\Gamma(1+2\,\alpha)}{\Gamma(1+\alpha)^2\,\Gamma(1+3\,\alpha)}\, I_t^{(3)}(T).
\end{aligned}
$$

In particular, we easily identify the pattern

$$
(X\diamond)^k M_t(T) = \frac{(\rho\,\nu)^k}{\Gamma(1+k\,\alpha)}\, I_t^{(k)}(T).
$$

## The leverage swap under rough Heston

Using (12), we have

$$
\begin{aligned}
\mathcal{L}_t(T) &= \sum_{k=1}^{\infty} (X \diamond)^k M_t(T) \\
&= \sum_{k=1}^{\infty} \frac{(\rho \nu)^k}{\Gamma(1 + k\alpha)} \int_t^T du\, \xi_t(u)\, (T - u)^{k\alpha} \\
&= \int_t^T du\, \xi_t(u)\, \{E_\alpha(\rho \nu \, (T - u)^\alpha) - 1\} \qquad (14)
\end{aligned}
$$

where $E_\alpha(\cdot)$ denotes the Mittag-Leffler function.

An explicit expression for the leverage swap!

## The normalized leverage swap

Given the form of equation (14), it is natural to normalize the leverage swap by the variance swap. We therefore define

$$L_t(T) = \frac{\mathcal{L}_t(T)}{w_t(T)}. \tag{15}$$

In the special case of the rough Heston model with a flat forward variance curve,

$$L_t(T) = E_{\alpha,2}(\rho \, \nu \, \tau^\alpha) - 1,$$

where $E_{\alpha,2}(\cdot)$ is a generalized Mittag-Leffler function. We further define an $n$th order approximation to $L_t(T)$ as

$$L_t^{(n)}(T) = \sum_{k=1}^{n} \frac{(\rho \, \nu \, \tau^\alpha)^k}{\Gamma(2 + k \, \alpha)}.$$

## A numerical example

We now perform a numerical computation of the value of the leverage swap using the forest expansion in the rough Heston model with the following parameters, calibrated to the SPX options market as of April 24, 2017:

$$H = 0.0236; \quad \nu = 0.3266; \quad \rho = -0.6510.$$

## The leverage swap under rough Heston

In Figure 12, we plot the normalized leverage swap $L_t(T)$ and successive approximations $L_t^{(n)}(T)$ to it as a function of $\tau$.
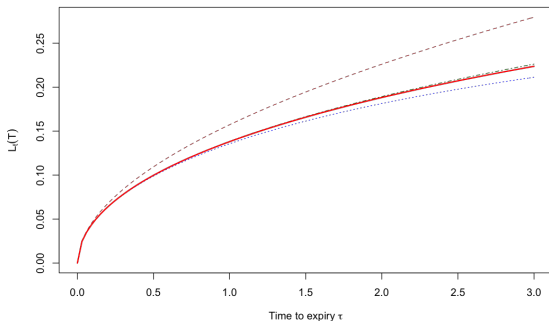


Figure 12: Successive approximations to the (absolute value of) the normalized rough Heston leverage swap. The solid red line is the exact expression $L_t(T)$; $L_t^{(1)}(T)$, $L_t^{(2)}(T)$, and $L_t^{(3)}(T)$ are brown dashed, blue dotted and dark green dash-dotted lines respectively.

## The leverage swap under rough Heston

We note that three terms are enough to get a very good
approximation to the normalized leverage swap for all expirations
traded in the listed market. Moreover, leverage swaps are
straightforward to estimate from volatility smiles.

### Remark

In practice, (15) can be used for very fast and efficient calibration
of the three parameters of the rough Heston model by minimizing
the distance between model and empirical normalized leverage
swap estimates.
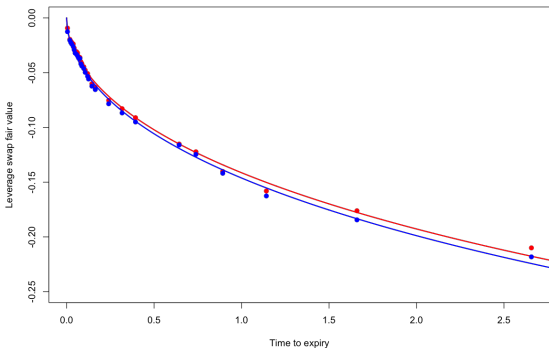
# Leverage estimates using VolaDynamics



Figure 13: Leverage estimates using the VolaDynamics curves C13PM (red) and C14PM (blue) and their respective rough Heston fits as of 24-Apr-2017. See https://voladynamics.com.

- With a good volatility surface parameterization, the term structure of normalized leverage can be robustly estimated.

## Summary

- We uncovered a remarkable monofractal scaling relationship in historical volatility which now appears to be universal.

- This leads to a natural non-Markovian stochastic volatility model under $\mathbb{P}$.

- The resulting volatility forecast beats existing alternatives.

- The simplest specification of $\frac{d\mathbb{Q}}{d\mathbb{P}}$ gives a non-Markovian generalization of the Bergomi model.
  - The history of the Brownian motion $\{W_s, s < t\}$ required for pricing is encoded in the forward variance curve, which is observed in the market.

- This model fits the observed volatility surface surprisingly well with very few parameters.

- Efficient calibration of the model to the volatility surface is now within reach.

# References

Elisa Alòs, Jorge A León, and Josep Vives.
On the short-time behavior of the implied volatility for jump-diffusion models with stochastic volatility.
*Finance and Stochastics*, 11(4):571–589, 2007.

Elisa Alòs.
A decomposition formula for option prices in the Heston model and applications to option pricing approximation.
*Finance and Stochastics*, 16(3):403–422, 2012.

Elisa Alòs, Jim Gatheral, and Radoš Radoičić.
Exponentiation of conditional expectations under stochastic volatility.
*SSRN*, 2017.

Emmanuel Bacry and Jean François Muzy.
Log-infinitely divisible multifractal processes.
*Communications in Mathematical Physics*, 236(3):449–475, 2003.

Emmanuel Bacry and Jean-François Muzy.
Hawkes model for price and trades high-frequency dynamics.
*Quantitative Finance*, 14(7):1147–1166, 2014.

Christian Bayer, Peter Friz, and Jim Gatheral.
Pricing under rough volatility.
*Quantitative Finance*, 16(6):887–904, 2016.

Lorenzo Bergomi and Julien Guyon.
Stochastic volatility's orderly smiles.
*Risk May,* pages 60–66, 2012.

Mikkel Bennedsen, Asger Lunde, and Mikko S Pakkanen.
Hybrid scheme for Brownian semistationary processes.
*Finance and Stochastics,* 21(4): 931-965, 2017.

Mikkel Bennedsen, Asger Lunde, and Mikko S Pakkanen.
Decoupling the short-and long-term behavior of stochastic volatility.
*Available at SSRN 2846756,* 2016.

Omar El Euch and Mathieu Rosenbaum.
The characteristic function of rough Heston models.
*arXiv preprint arXiv:1609.02108,* 2016.

Masaaki Fukasawa.
Asymptotic analysis for stochastic volatility: Martingale expansion.
*Finance and Stochastics,* 15(4):635–654, 2011.

Masaaki Fukasawa.
The normalizing transformation of the implied volatility smile.
*Mathematical Finance,* 22(4):753–762, 2012.

Jim Gatheral.
*The volatility surface: A practitioner's guide.*
John Wiley & Sons, 2006.

Jim Gatheral, Thibault Jaisson, and Mathieu Rosenbaum.
Volatility is rough.
*Quantitative Finance*, forthcoming, 2018.

Thibault Jaisson and Mathieu Rosenbaum.
Rough fractional diffusions as scaling limits of nearly unstable heavy tailed Hawkes processes.
*The Annals of Applied Probability*, 26(5):2860–2882, 2016.

Ryan McCrickerd and Mikko S. Pakkanen
Turbocharging Monte Carlo pricing for the rough Bergomi model.
*arXiv preprint arXiv:1708.02563*, 2017.

Carl J Nuzman and Vincent H Poor.
Linear estimation of self-similar processes via Lamperti's transformation.
*Journal of Applied Probability*, 37(2):429–452, 2000.